Fast Implementation of New S-Band Capability in the Deep Space Network

Jose E. Velazco,* John Sosnowski,* Jim Bowen,* Ted Hanson,* Juan Ocampo,* John Huleis,* Mark Taylor,* Erick Pereira,* Steve Montanez,* Michael Young,* Chris Link,* Ezra Long,* Hungsheng Lin,* and Manuel Franco*

ABSTRACT. — We report on the implementation of a new S-band (2025–2120 MHz uplink, 2200–2300 MHz downlink) communications system capability for the Deep Space Network's (DSN) Deep Space Station 36 (DSS-36) performed by JPL's Communications Ground Systems Section (333). The newly implemented S-band system, consisting of a transmitter, a receiver, a waveguide system, and a feed, will enhance the capabilities of NASA's DSN to communicate with spacecraft in near-Earth orbit. A key milestone achieved during this project, described in detail in this article, is the implementation of an S-band receiver that features the best sensitivity to date in the DSN S-band systems. It is noteworthy that, in order to alleviate scheduling issues associated with installation of other systems into DSS-36, this successful implementation was carried out in record time.

I. Introduction

The Deep Space Network (DSN) provides telemetry, spacecraft commanding, and tracking to most of the robotic spacecraft in deep space and in some cases to the International Space Station and near-Earth flight missions. The DSN provides the aforementioned communications services via three Deep Space Communications Complexes (DSCCs) located, respectively, in California (Goldstone), Spain (Madrid), and Australia (Canberra). Each DSCC currently includes one 70-m, one 34-m high-efficiency (HEF), and several newer 34-m beam-waveguide (BWG) deep space stations (DSS).[1] Within the next decade, NASA plans to gradually retire the 70-m and HEF antennas and to have implemented a total of five BWG stations per complex for a total of 15 stations across the network.[2] Currently, three of the existing BWG stations and three of the HEF stations possess S-band link capabilities (one of each at each complex) and NASA would like to at least maintain this S-band capacity to cope with current and future near-Earth S-band communications demands. Furthermore, due to the HEFs' obsolescence, NASA plans to gradually decommission them at the rate of one station per year starting in 2016. Part of this planning considers recycling the S-band systems from the three retiring HEF stations and installing them into three current BWG

* Communications Ground Systems Section.

[1] Deep Space Network Complexes — http://deepspace.jpl.nasa.gov/about/DSNComplexes/#

[2] Deep Space Network Aperture Enhancement Project (DAEP) — http://www.nasa.gov/directorates/heo/scan/services/networks/txt_daep.html

The research described in this publication was carried out by the Jet Propulsion Laboratory, California Institute of Technology, under a contract with the National Aeronautics and Space Administration.

stations that do not possess this capability. Consequently, by 2020 NASA's goal is to retire all the HEF stations and to have two BWG stations with S-band capability at each DSCC.

The planned BWG DSS stations to be furnished with new S-band capability are DSS-36, DSS-26, and DSS-56. DSS-26 is an existing station located at Goldstone, DSS-36 is currently under construction in Canberra and is scheduled to start operations in October 2016, and DSS-56 will be constructed in Spain with scheduled start of operations in 2019.

In order to maintain dual S-band capability in each of the three DSN complexes while we gradually decommission the HEF stations, the goal is to start the BWG S-band implementation process by using the first S-band system from station DSS-27, which was previously decommissioned in 2014. To clarify this round-robin process, Figure 1 shows the origin and target stations for the various S-band systems to be implemented under this program. DSS-36 will receive the S-band system from DSS-27, DSS-26 from DSS-45, and DSS-56 from DSS-15. The S-band system parts from DSS-65 will be used as spares.

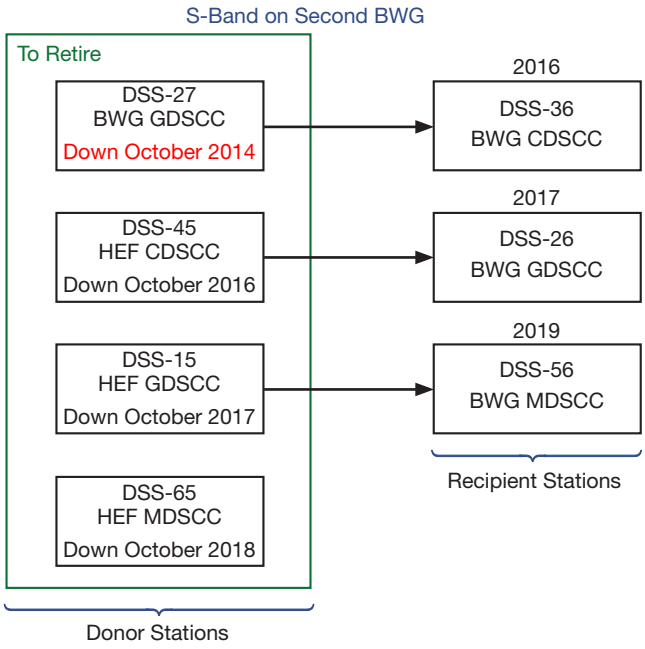

Figure 1. Diagram showing the new S-band implementation process across the DSN.

In March 2015, we started the S-band recycling process. This involved refurbishing parts from DSS-27 with the initial goal of installing the upgraded S-band system into DSS-36 18 months later, namely by August 2016. This article presents the status of that implementation effort.

II. S-band Implementation for DSS-36

DSS-36 is a new 34-m BWG station that will have S-, X-, and Ka-band communication capabilities. It is scheduled to start operations in October 2016. Figure 2 shows the entire DSS-36 BWG station, including the location of the S-band system (below M6), mirrors, and reflector.

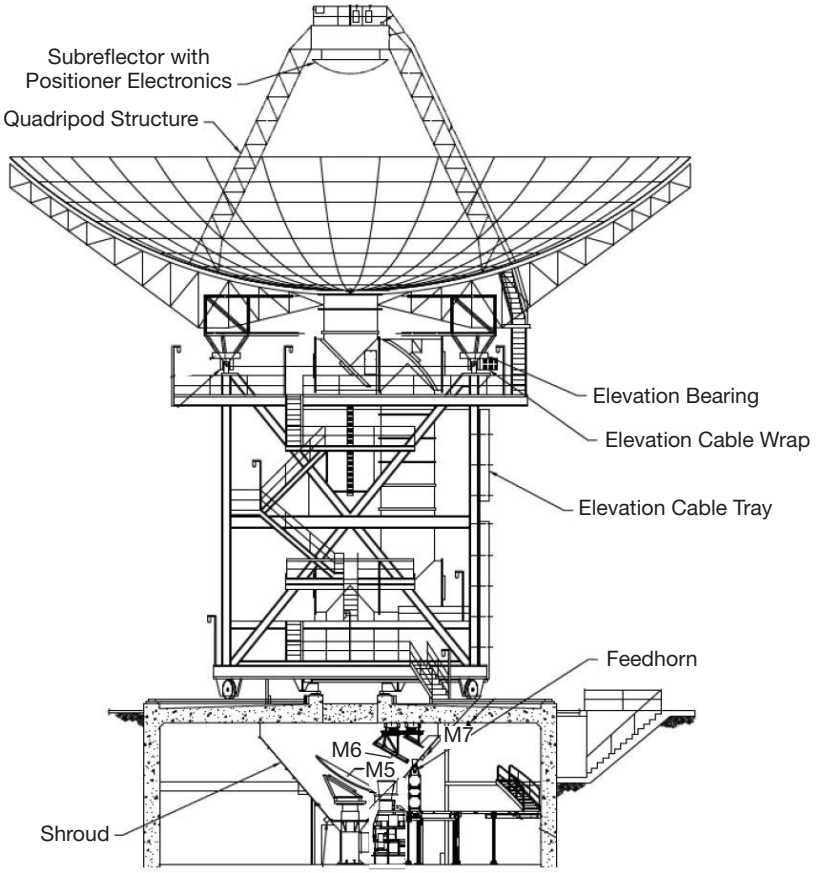

Figure 2. DSS-36 beam-waveguide schematic.

The S-band system to be implemented in DSS-36, shown schematically in Figure 3, consists of uplink, downlink, and feed subsystems. Other S-band subsystems such as downconverters and exciter are not covered in this article. Consequently, in the remainder of this article we shall concentrate on discussing the implementation status of the low-noise amplifier system (downlink), the transmitter (uplink), waveguide system, and feed. The uplink components include a 250-W transmitter, RF switch, RF load, and filter. The downlink includes the receiver filter, RF switch, RF load, and cryogenic high-electron-mobility-transistor (HEMT) low-noise amplifier (LNA). The polarizer, diplexer, and RF switch make up the waveguide system.

It should be pointed out that, in coordination with the sponsoring office, it was agreed to accelerate the delivery of this system by six months in order to not interfere with the installation of the X- and Ka-band communication systems into DSS-36. Consequently, the delivery date for the S-band system was shortened by six months and switched from August 2016 to March 2016.

The specific goals of this effort were to:

(1) Move the S-band system from DSS-27 (Goldstone) to JPL.

(2) Design a new mechanical supporting frame.

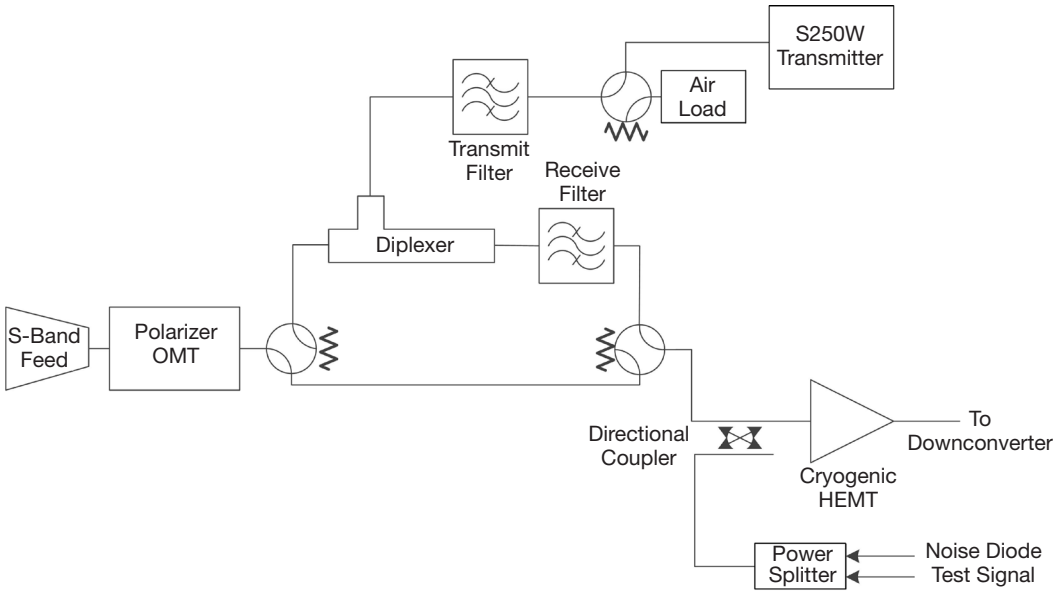

Figure 3. Schematic of S-band system.

(3) Reuse the feed from DSS-27.

(4) Reuse most of the waveguide components and acquire the interconnecting waveguides.

(5) Design a new LNA package (downlink).

(6) Reuse the transmitter (uplink).

(7) Perform testing of the subsystems.

(8) Perform final testing of the entire S-band system.

The target operational parameters of the S-band system described here are shown in Table 1.

Table 1. S-band system parameters.

Item	Symbol	Value
Frequency Range		
Uplink	—	2025–2120 MHz
Downlink	—	2200–2300 MHz
Uplink Transmit Power	—	250 W
LNA Noise Temperature	T_{LNA}	6.1 K
Operational Noise Temperature	T_{op}	31 K
Gain Over System Temperature	G/T_{op}	42 dB

A. New Mechanical Frame

In order to assemble the entire upgraded S-band system, a new mechanical supporting frame was designed. This frame houses the feed, LNA package, and waveguide system. The requirements for this new frame design included: accurate adjustment in all directions, compact and lightweight, easy to transport and install, capable of accepting both future and old diplexers, and able to be installed in future and current BWG antennas (i.e., DSS-24/25/26/34/35/54/55).

The main features of the new frame are: slotted brackets that allow for 0.5 in. adjustment in all directions, simple box design, lightweight aluminum build, use of steel footplates that protect aluminum from grout and allow vertical adjustability, and compact design that takes up less than half the space of previous design.

The complete S-band system (including its new frame) is installed in the BWG station's pedestal in the manner shown in Figure 4. The frame design used for installation of S-band systems into HEF stations was initially considered for this new implementation (hereafter referred to as the original frame). The original frame base was fairly large and presented several height adjustment mechanisms that made it overly complicated for the current implementation.

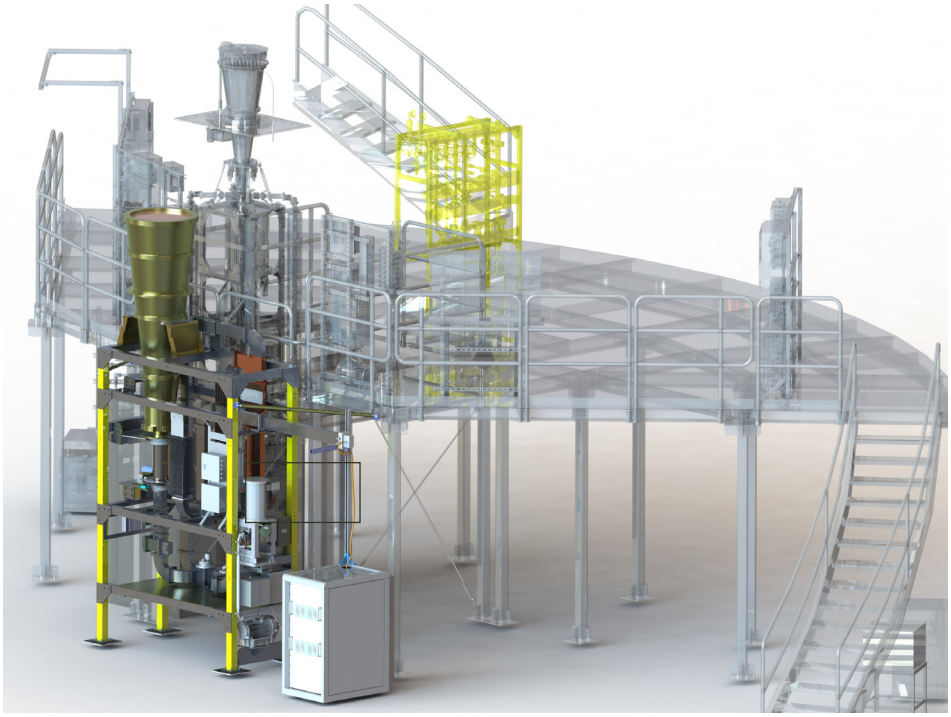

Figure 4. Schematic showing the S-band system installed in the pedestal of station DSS-36.

During the S-band layout process, the original frame layout was placed in our SolidWorks antenna model along with the main platform to determine possible areas of interference (see Figure 5).

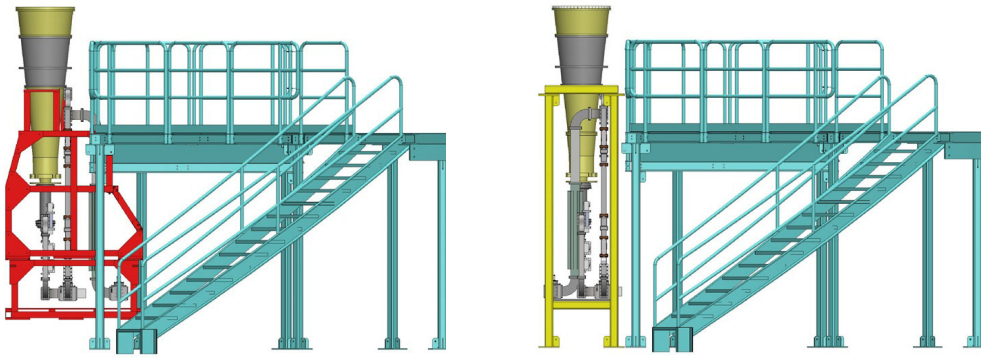

Figure 5. Images showing (a) the original frame (in red) and (b) the new frame (in yellow).

Upon inspection, it was apparent that the original frame was not suitable for this application due to mechanical interference with the main platform. Furthermore, during this study it was also discovered that part of the S-band waveguide system would overlap with the main platform. Consequently, it was decided that a new frame had to be implemented and that the interfering waveguide parts had to be rerouted to clear the platform.

The CAD software SolidWorks was used exclusively in the design of the frame and for structural analysis. A bolted frame design was pursued to allow flexibility for design changes. The design philosophy of the new frame dictated that the entire populated frame was to be crated and shipped without being disassembled. This constraint required that the populated frame be capable of supporting its own weight while being lowered to a horizontal position. Cross members and brackets were implemented into the design so as to support the frame hardware in any position.

The upper feedhorn sections are shipped separately and installed after the frame is in its final location. A lifting fixture/shipping cage was designed to provide a hoisting lug and protect the exposed components during shipment. The estimated hoisting weight for this frame was 2,200 lb. Figure 6 shows a SolidWorks image of the finalized new frame, including all the S-band components.

B. Uplink

The uplink of the S-band system, shown schematically in Figure 7, has the purpose of delivering the desired S-band signal to the spacecraft. It consists of power supplies, solid-state power amplifiers, control boxes, etc. The uplink is designed to deliver 250 W across the 2025–2110 MHz band. It receives a low-power (10-mW) signal from the exciter (whose level can be adjusted via a variable attenuator), is amplified to 2 W, and finally is boosted by a solid-state amplifier to a power of 250 W. The output of the solid-state amplifier is a type-N coaxial connector. A 1-m low-loss RG-58 coaxial line connects the solid-state amplifier to a coaxial-to-waveguide adapter. In previous designs, the adapter was directly connected to a straight piece of waveguide. However, in this S-band implementation we include a new power monitoring system, wherein the adapter is connected to a dual directional coupler and then to the straight waveguide (see Figure 7). The outputs of the directional coupler

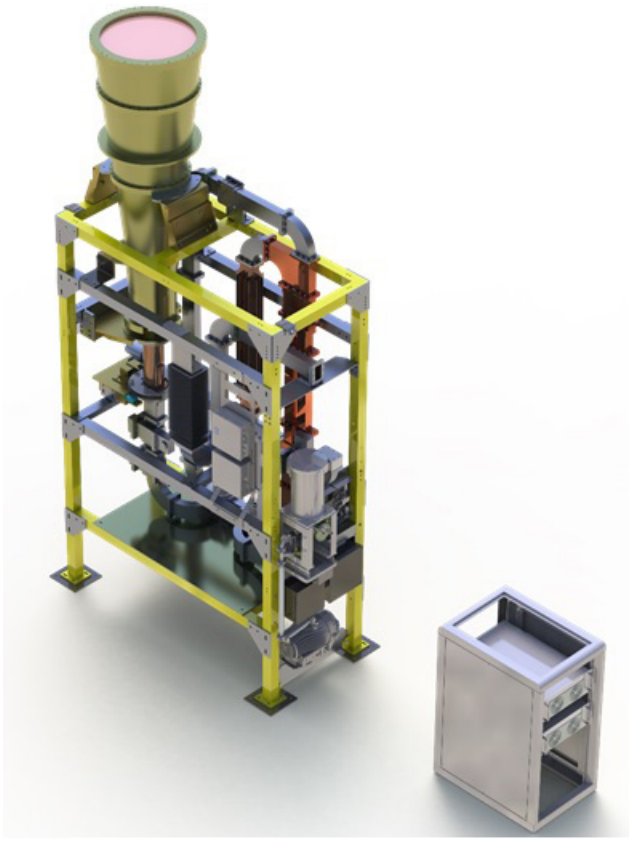

Figure 6. Drawing showing the new S-band frame (yellow).

are used to monitor forward and reflected power at that point using a dual-channel power meter.

The high-power 250-W signal is then sent to the feed for radiation into the BWG mirror structure for radiation into space.

The entire uplink system was assembled inside a new rack in the configuration shown in Figure 8. Subsequently, the uplink system was thoroughly tested to determine gain and stability according to the DSN standards.[3] Plots of output power as a function of frequency are shown in Figure 9. Note that stable 250-W output power is obtained.

C. Waveguide System and Feed

The waveguide system, shown in Figure 10, is employed to connect the uplink and downlink systems with the feed. It consists of a filter, diplexer, switches, and segments of rectangular waveguide. During this project, we recycled various waveguide parts from DSS-27 and procured additional components such as RF switches. All these parts were independently tested and subsequently assembled together. After being assembled, the waveguide system was tested for insertion loss, which was measured to be $T_{UWV} = 2$ K.

[3] *Uplink Tracking and Command Subsystem Functional Requirements*, DSN No. 834-077 (internal document), Jet Propulsion Laboratory, Pasadena, California, p. 62.

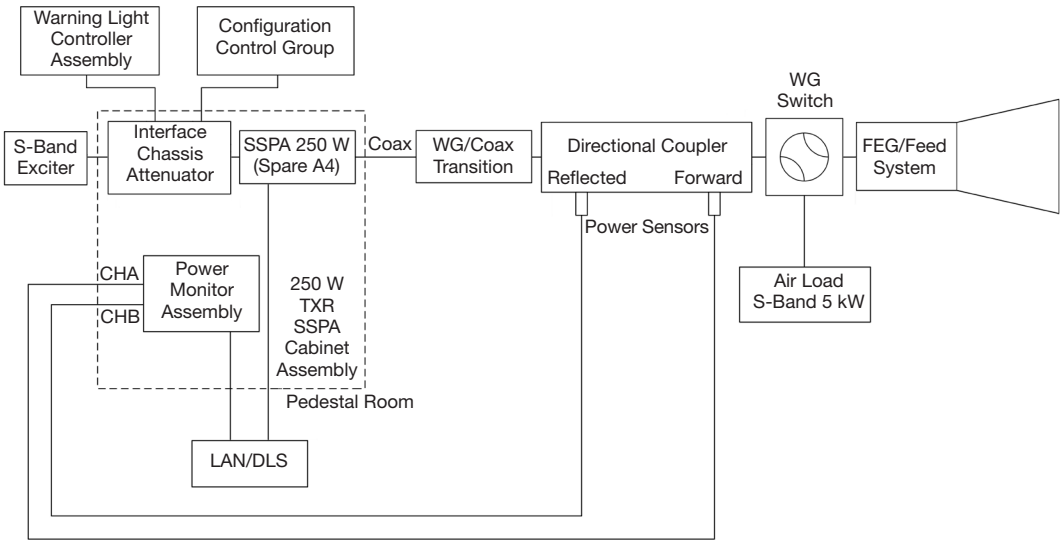

Figure 7. Schematic of S-band uplink system.

Figure 8. Picture of the S-band uplink rack including power monitoring and 250-W solid-state amplifier assemblies.

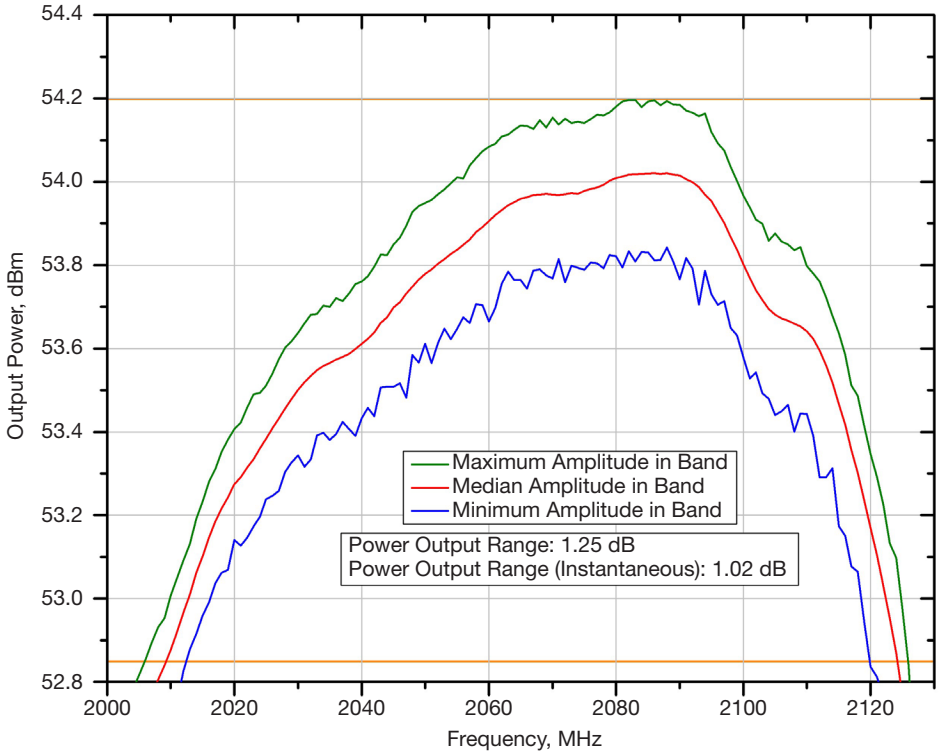

Figure 9. Plots of output power as a function of time (frequency) are shown.

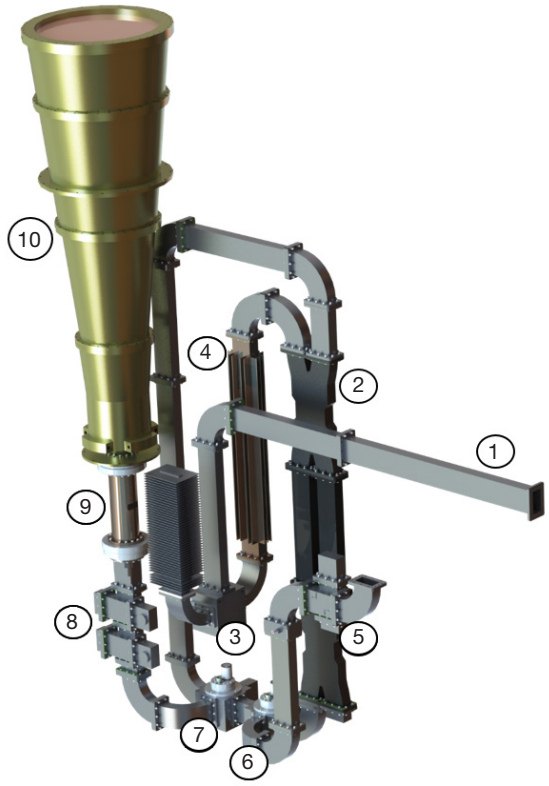

Figure 10. Drawing showing the various S-band waveguide components: ①straight waveguide, ②diplexer, ③⑥⑦RF switch, ④filter, ⑤coupler, ⑧directional coupler, ⑨polarizer, ⑩feed.

The feed employed in this implementation is a corrugated feed with a flare angle of 6.7 deg and length of 58 in. The feed, shown in Figure 10 (item 10), consists of three sections and provides a gain of 20 dB.

D. Downlink System

The S-band downlink system described here consists of a cryocooled low-noise amplifier package (see Figure 11). The critical item within the LNA system is the low-noise amplifier module. The downlink system has the challenge of being able to receive picowatt-level signals coming from spacecraft in deep space and amplifying them to suitable power levels so that they can be further processed.

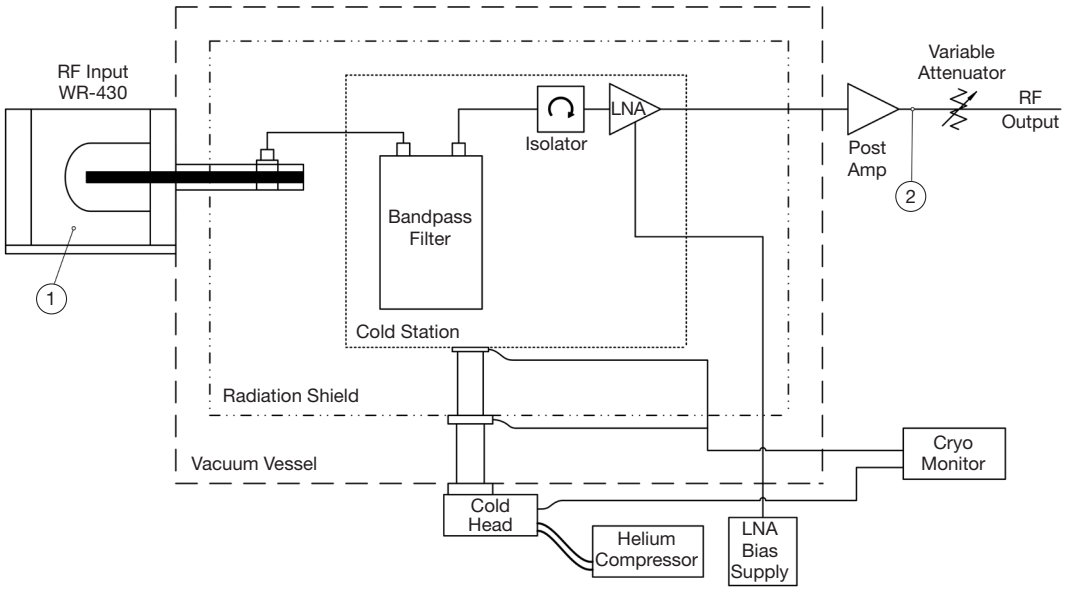

Figure 11. Schematic of S-band downlink system.

During this effort, we built a new LNA cryo package that consisted of a dewar, cold head, compressor, and microwave string. The microwave string includes a cold finger (coax-to-waveguide adaptor), bandpass filter, isolator, and LNA module. A key effort in this project was the investigation of various LNA modules that were available on the market. We tested S-band LNAs from Caltech, National Radio Astronomy Observatory (NRAO), and Low Noise Factory (LNF). The Caltech model LF3 includes three silicon germanium (SiGe) LNAs made from discrete transistor chips fabricated by ST Microelectronics in France. NRAO's LNA modules use single-ended cryo3 indium phosphide (InP) LNA chips that were provided by JPL. Testing of these devices was performed in two stages. First, we tested the LNA modules inside our cryogenic testbed to determine noise temperature, gain, and device stability. For the second test, we attached the LNA cryo package to a suitable feed in our rooftop laboratory to measure noise temperature of the entire system, including the feed. We used our typical test setup to perform testing of the LNA modules, which involves adding an isolator in front of the device under test. Figure 12 shows a picture of the LNA module and isolator inside the cryogenic package. The vacuum vessel is pumped to a vacuum level of 10^{-3} Torr and subsequently cooled down to a physical temperature of 15 K using a two-stage CTI-Cryogenics Gifford McMahon (GM) helium cryogenic refrigerator. Gain measurements were performed via ports 1 and 2 (see Figure 11) using a network analyzer. Noise temperature

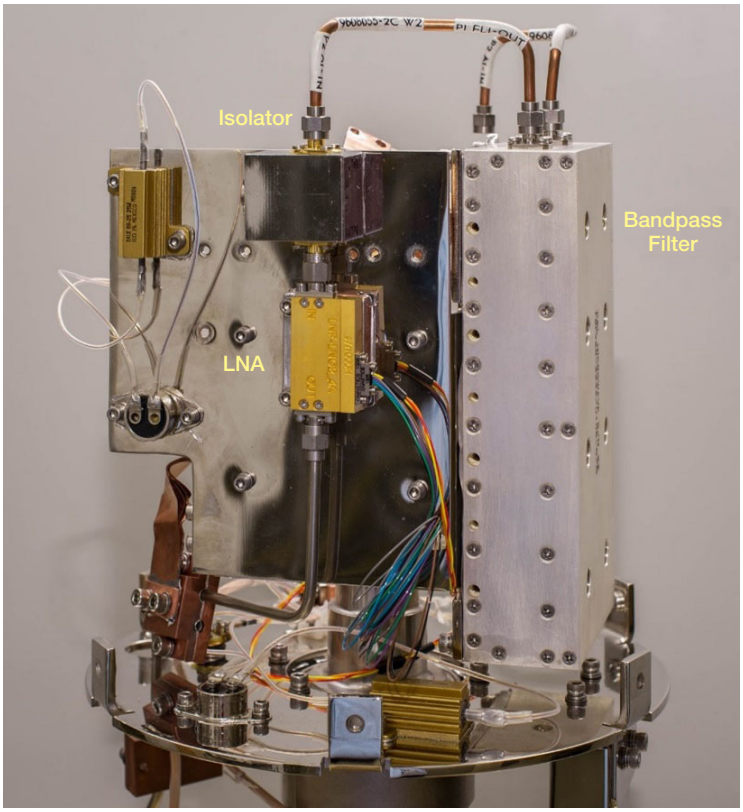

Figure 12. Picture of LNA module and associated isolator.

performance of the LNA system was measured at port 2 using a spectrum analyzer. We used properly calibrated diode temperature sensors placed on the LNA body to measure physical temperature of the LNA. Figure 13 shows noise temperature measurements of the various LNAs tested with our rooftop testbed. In these measurements, the LNA noise temperature was obtained by removing the contributions from the feed. Note that the best result of 3.5 K was obtained with LNAs from Low Noise Factory.

E. Noise Temperature Measurements

The various noise temperature values throughout the S-band system, shown in Figure 14, include the LNA package noise T_{LNA}, the waveguide system noise T_{WVG}, the feed noise T_{feed}, and the microwave noise T_{UWV}. All these values are related by

$$T_{UWV} = T_{LNA} + T_{WVG} + T_{feed}\,. \tag{1}$$

T_{LNA} is the noise temperature measured at the output window of the LNA package (port 1 in Figure 11), and includes contributions of the LNA modes plus other circuitry inside the package. T_{WVG} consists of the noise temperature contributions of the waveguide system. T_{feed} is the noise added by the feedhorn, whereas T_{UWV} is the noise temperature measured at the feedhorn output plane and includes the noise contribution of the entire downlink hardware below that plane. DSN guidelines dictate a maximum microwave noise temperature, T_{UWV}, of 12 K.[4]

[4] *DSN Microwave Subsystem (UWV) Requirements*, DSN No. 834-016 (internal document), Jet Propulsion Laboratory, Pasadena, California, p. 76.

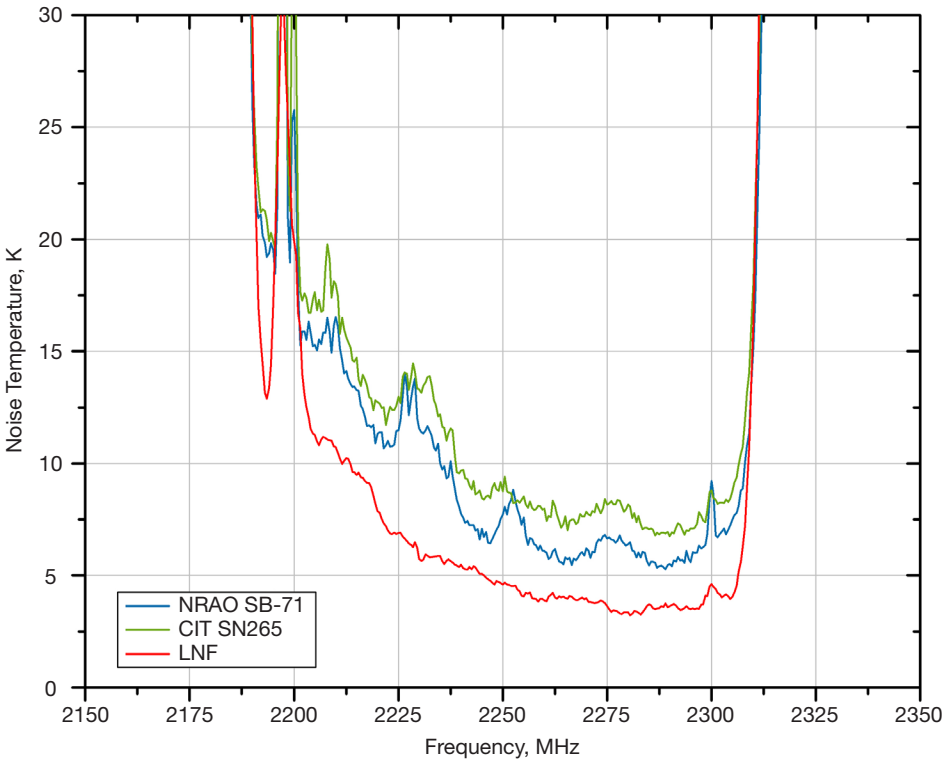

Figure 13. Noise temperature measurements of the three LNA modules are shown as a function of frequency.

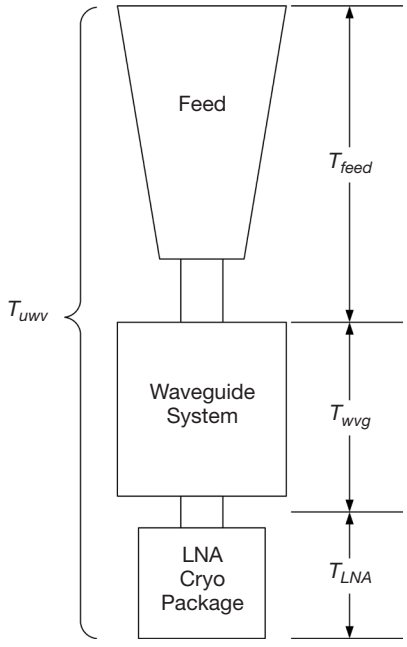

Figure 14. S-band block diagram showing location of various noise temperature planes.

The operation noise temperature of the antenna, T_{op}, is related to T_{uwv} by

$$T_{op} = T_{UWV} + T_{ANT} + T_{SKY} \tag{2}$$

where $T_{ANT} = 14.5$ K[5] is the noise contribution of the antenna (including the BWG mirrors) and T_{SKY} is the sky noise temperature contribution (atmospheric and cosmic microwave background noise). T_{SKY} is typically 4.8 K at GDSCC. Therefore, assuming a $T_{UWV} = 12$ K,[6] the expected operation temperature for the S-band system is $T_{op} = 31.3$ K.

F. Testing of Entire System

Once we successfully tested all the subsystems, the entire S-band system was assembled inside its new frame, as shown in Figure 15. Subsequently, the system was moved next to building 149 at JPL, where the required power and cooling lines were set up and the system

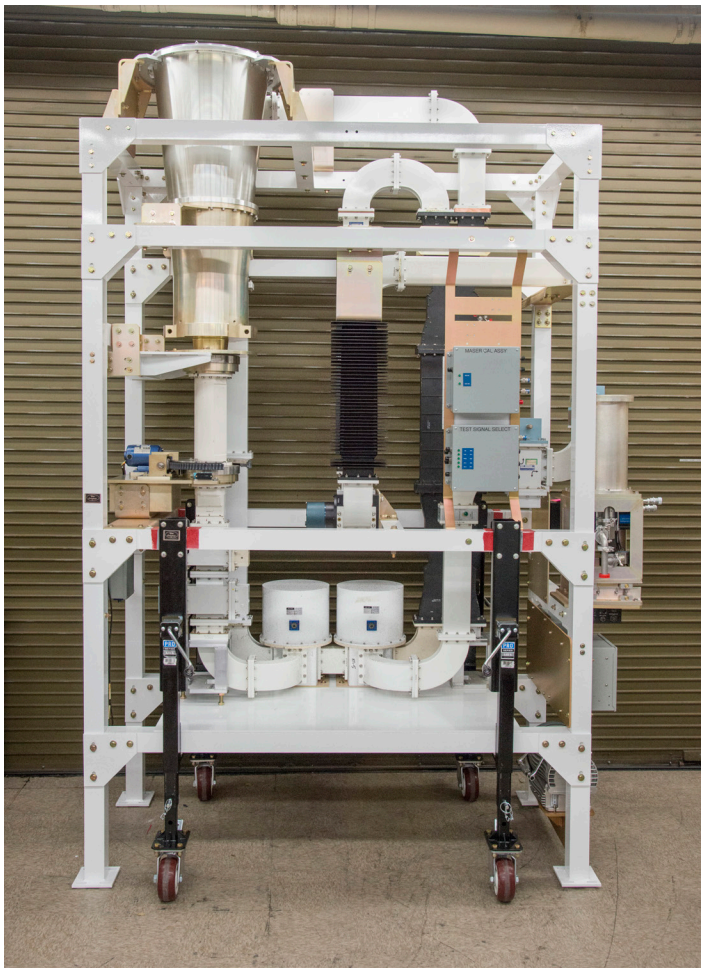

Figure 15. Picture of the S-band system including its new frame and various components.

[5] *Antenna Microwave System Functional Requirements and Design*, DSN No. 828-007 (internal document), Jet Propulsion Laboratory, Pasadena, California.

[6] *DSN Microwave Subsystem (UWV) Requirements*, DSN No. 834-016 (internal document), Jet Propulsion Laboratory, Pasadena, California, p. 76.

was thoroughly tested. In Figure 16, we show a picture of the entire S-band system under testing. The system successfully passed all the required testing. It should be pointed out that the measured noise temperature is represented by Equation (2)minus the antenna contribution ($T_{ANT} = 14.5$ K). Noteworthy is the fact that the measured operational temperature was $T_{UWV} + T_{SKY} = 13$ K, which represents a record performance of any S-band system currently in operation in the DSN. Including the $T_{ANT} = 14.5$ K antenna noise contribution yields an antenna $T_{op} = 27.5$ K. Table 2 lists operational noise performance of all S-band systems in the DSN[7] [1], demonstrating that the newly implemented system at DSS-36 features the best noise temperature of all current systems.

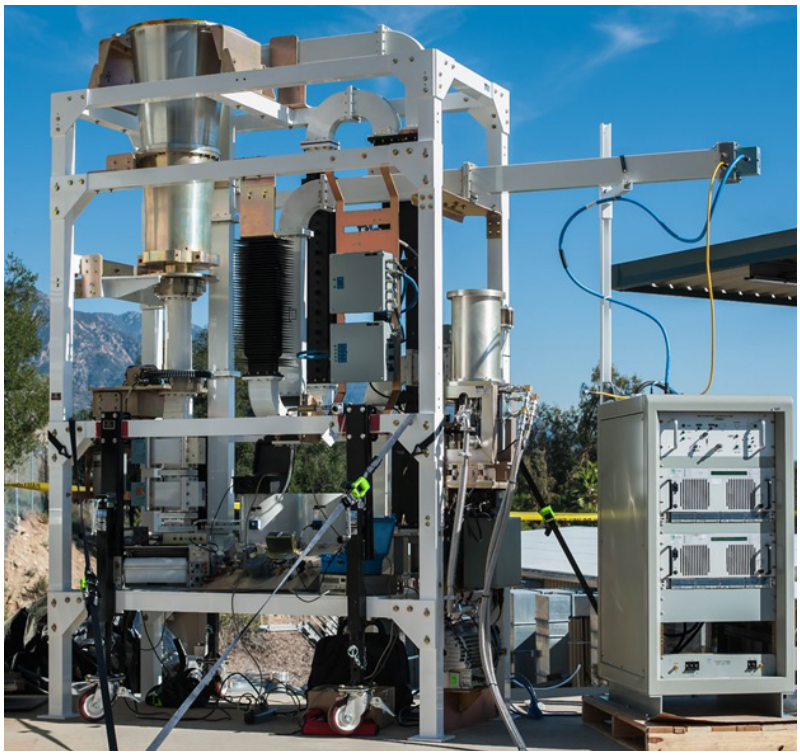

Figure 16. Picture of the S-band system after successfully testing.

Table 2. Operational noise temperature T_{op} performance of S-band systems in the DSN.

Antenna	Symbol	Value
DSS-15	K	38.8
DSS-45	K	—
DSS-65	K	—
DSS-24	K	31.3
DSS-34	K	32
DSS-54	K	28.4
DSS-36	K	27.5

[7] *Antenna Microwave System Functional Requirements and Design*, DSN No. 828-007 (internal document), Jet Propulsion Laboratory, Pasadena, California.

III. Conclusions

A new S-band communications system for the DSN was successfully assembled and tested in record time. The S-band system implemented under this project will become part of DSS-36 in the Canberra DSCC. Despite reducing the delivery schedule by almost half a year, the system was successfully implemented and tested and the delivery was on budget. Noteworthy is the fact that the tested system features the best sensitivity to date of all the S-band systems within the DSN.

References

[1] S. D. Slobin, "34-m BWG Station Telecommunications Interfaces," *DSN Telecommunications Link Design Handbook*, DSN No. 810-005, Space Link Interfaces, Module 104, Rev. H, Jet Propulsion Laboratory, Pasadena, California, March 5, 2015. http://deepspace.jpl.nasa.gov/dsndocs/810-005/104/104H.pdf